# Chapter 18
# Hypoxia Imaging with $^{18}$F-FMISO PET for Brain Tumors

**Kenji Hirata, Kentaro Kobayashi, and Nagara Tamaki**

**Abstract** Tumor hypoxia is an important object for imaging because hypoxia is associated with tumor aggressiveness and resistance to radiation therapy. Here, $^{18}$F-fluoromisonidazole (FMISO) has been used for many years as the most commonly employed hypoxia imaging tracer. Unlike F-18 fluorodeoxyglucose (FDG), FMISO does not accumulate in normal brain tissue making it able to provide images of hypoxic brain tumors with high contrast. Clinical evidence has suggested that FMISO PET can predict patient prognosis and treatment response. Among gliomas of various grades (WHO 2007), it has been known that grade IV glioblastoma resides under severe hypoxia and is a cause of development of necrosis in the tumor. For this study we tested whether FMISO can distinguish the oxygen condition of glioblastomas and lower-grade gliomas. Twenty-three glioma patients underwent FMISO PET for the study. All the glioblastoma patients ($N = 14$) showed high FMISO uptakes in the tumor, whereas none of the other patients (i.e., gliomas of grade III or lower, $N = 9$) did, demonstrated by both qualitative and quantitative assessments. The data suggest that FMISO PET may be a useful tool to distinguish glioblastomas from lower-grade gliomas. Our results, however, were slightly different from previous investigations reporting that some lower-grade gliomas (e.g., grade III) showed positive FMISO uptake. Many of these acquired the FMISO PET images 2 h after the FMISO injection, while for the study here we waited 4 h to be able to collect hypoxia-specific signals rather than perfusion signals as FMISO clearance from plasma is slow due to its lipophilic nature. No optimum uptake time for FMISO has been established, and we directly compared the 2-h vs. the 4-h images with the same patients ($N = 17$). At 2 h, the gray matter had significantly higher standardized uptake value (SUV) than the white matter, possibly due to different degrees of perfusion but not due to hypoxia. At 4 h, there were no differences between gray and white matter without any significant increase in the noise level measured by the coefficient of variation between the 2-h and the 4-h images. At 2 h, 6/8 (75 %) of glioblastoma patients

K. Hirata (✉) • K. Kobayashi
Department of Nuclear Medicine, Hokkaido University, Sapporo, Japan
e-mail: khirata@med.hokudai.ac.jp

N. Tamaki
Department of Nuclear Medicine, Graduate School of Medicine, Hokkaido University, Sapporo, Japan



Y. Kuge et al. (eds.), *Perspectives on Nuclear Medicine for Molecular Diagnosis and Integrated Therapy*, DOI 10.1007/978-4-431-55894-1_18

showed higher uptakes in the tumor than in the surrounding brain tissue, whereas at 4 h this was the case for 8/8 (100 %). In addition, at 2 h, 3/4 (75 %) of patients with lower-grade gliomas showed moderate uptakes, while at 4 h none did (0/4 or 0 %). These data indicate that 4-h images are better than 2-h images for the purpose of glioma grading. In conclusion, we evaluated the diagnostic performance of FMISO PET for gliomas and suggest that FMISO PET may be able to assist in the diagnosis of glioblastomas when PET images are acquired at 4 h post injection.

**Keywords** Hypoxia • 18 F-Fluoromisonidazole • Glioma • Glioblastoma

## 18.1 Introduction

This review article summarizes our recent studies with $^{18}$F-fluoromisonidazole (FMISO) positron emission tomography (PET) applied to brain tumors [1, 2]. A variety of tumors which can be divided into two categories develop in the brain: primary brain tumors that originate from the brain tissue and metastatic brain tumors that originate from malignant tumors in other organs. Gliomas account for 60 % of primary brain tumors. Gliomas comprise a range of tumors, from benign to malignant, that are derived from glial cells such as astrocytes, oligodendrocytes, and ependymal cells. Among gliomas, the glioblastoma is the most aggressive astrocytic tumor. Glioblastomas are categorized as grade IV in the WHO classification [3]. The standard treatment for glioblastomas is surgery followed by radiotherapy and chemotherapy [4]. With state-of-the-art multidisciplinary therapy, the 1-year survival rate of glioblastoma patients is reported to be 56 %, which is significantly poorer than with grade III (78 %) or less malignant gliomas [5]. A pathological diagnosis of surgical specimens by biopsy or resection is necessary to establish the diagnosis for glioblastomas [6], but brain surgery involving eloquent regions can exacerbate the prognosis by causing neurological morbidity and should be avoided if possible [7]. Patients with impaired performance status or elderly patients especially would benefit from nonsurgical methods of establishing the diagnosis, substituting surgical tissue sampling.

The basic in vivo imaging modality for brain tumors is magnetic resonance (MR) imaging. Intratumoral characteristics and tumor expansion states are shown accurately with MR imaging. The use of PET with $^{18}$F-fluorodeoxyglucose (FDG) is a well-established method for many different types of tumors in the body, including lung cancer, head and neck cancers, and others. FDG PET also plays important roles in the diagnosis of glioblastomas. The diagnosis of a glioblastoma is generally suggested if there is a ringlike enhancement by gadolinium on MR images or an intense uptake of FDG [6, 8–15]. However, there are cases of false-negative MRI findings as some glioblastoma lack the ringlike enhancement [6]. In discriminating glioblastoma from grade III tumors, FDG PET is also not always adequate as a large number of patients of grade III gliomas show high FDG uptakes [13, 14]. This makes a biopsy necessary in many cases, and a noninvasive in vivo imaging tool would be of benefit to omit invasive biopsy procedures in clinical settings [11].

The WHO 2007 criteria determine the glioma grade based on microscopic characteristics present in the malignancy. Grade II tumors show cell atypia and grade III tumors tissue anaplasia and cell mitosis in addition to cell atypia. Grade IV glioblastomas have pathological features that are not found in grade III or lower-grade gliomas, particularly microvascular proliferation and necrosis [3]. Basically, necrosis is considered to be closely related to hypoxia as low oxygen concentrations do not allow the energy metabolism to proceed as in unaffected tissue. In fact, glioblastomas are known to be in a state of severe hypoxia possibly due to vascular abnormalities and high oxygen demand, whereas the hypoxia of grade III or lower-grade gliomas is less severe [16–19]. We hypothesized that imaging the hypoxia of glioblastomas could be useful to distinguish glioblastomas from lower-grade gliomas.

Measuring hypoxia in living tissue uses needle electrodes; however, this technique presents significant shortcomings. First, it is invasive to insert a needle into deep layers of tissue in humans. Second, it requires considerable skill and the reproducibility is not high. Third, needles may alter the tissue structure and so influence the local oxygen partial pressure, and for these reasons needle electrodes are not used in clinical practice. An alternative is presented by $^{18}$F-fluoromisonidazole (FMISO) PET which is a widely used method for in vivo hypoxia imaging [20–23]. Valk et al. first introduced the use of FMISO for glioma imaging in 1992 [24], and the usefulness of FMISO for glioma imaging has been extensively investigated [25–32]. The FMISO is also known to accumulate in severe hypoxic structures but not in mildly hypoxic structures, suggesting that FMISO would be able to discriminate severe from mild hypoxia. This made us hypothesize that much FMISO may accumulate in glioblastomas and only little in lower-grade gliomas. If such a difference could be substantiated, hypoxia imaging using FMISO would provide an avenue to discriminate glioblastomas from lower-grade gliomas. The first paper of our project was to test the hypothesis [1]. We evaluated the diagnostic usefulness of FMISO PET in terms of glioma grading in comparison with diagnosis with FDG PET in patients suspected of having glioblastomas on MR images.

With FMISO there is a trade-off problem regarding uptake time (the interval between the FMISO injection and the PET emission scanning). A longer uptake time is theoretically desirable to image hypoxia with good lesion-to-background signal ratios, but the longer time leads to lower signal-to-noise ratios due to radiological decay of the F-18. Early reports by Grunbaum et al. [33] and Thorwarth et al. [34] addressing this issue suggested a 4-h acquisition as suitable. Despite this, most research adopted 2-h protocols [24, 25, 27–32], possibly because a shorter protocol would be more generally acceptable in clinical settings. Based on this, the second part of our project was to directly compare 2-h and 4-h images from the same patients [2].

## 18.2 Materials and Methods

The first of the studies reported here was conducted for the purpose of testing the ability to discriminate between glioblastomas and lower-grade gliomas with FMISO PET. Twenty-seven patients with possible high-grade gliomas were considered for the study [1]. The patients included showed cerebral parenchymal tumors surrounded by edematous tissue on MR images but no known malignancy in other organs. We excluded patients where previous tumorectomy, chemotherapy, or radiotherapy for lesions had been performed. The only exception was a patient with a recurrent tumor 6 years after tumorectomy combined with chemoradiotherapy for a low-grade glioma. Among the 27 patients, two were excluded because they had contraindications of surgical operations. The remaining 25 patients underwent either a tumoral resection ($n = 16$) or biopsy ($n = 9$) at most 2 weeks after the PET scanning. The surgical specimen was investigated by two experienced neuropathologists to determine the pathological diagnosis based on the 2007 WHO classification. Among the 25 patients, two were diagnosed as having metastatic adenocarcinoma and multiple sclerosis, respectively, and these two patients were excluded from the analysis. Finally 23 patients (M/F = 10:13, age $57 \pm 15$ years old) all with the pathological diagnosis of gliomas were included in the study.

With these 23 patients, we acquired FMISO and FDG PET images following the same protocol for all the patients. The interval between FMISO and FDG was at most 1 week. The FMISO synthesis protocol was previously described in detail elsewhere [35, 36]. On the day of FMISO, the patient was not asked to fast before the PET, and 400 MBq of FMISO was intravenously injected. Then, 4 h later, the emission scanning was initiated to acquire static PET images of the entire brain. FDG PET was performed on another day; here the dosage of FDG was also 400 MBq. The uptake time for FDG was 1 h, and the scanning range for the FDG PET was the same for the FMISO PET with a high-resolution PET scanner (ECAT HR+ scanner; Asahi-Siemens Medical Technologies Ltd., Tokyo, Japan) operated in a three-dimensional mode for 22 patients. For one patient the FMISO images were acquired using an integrated PET-CT scanner (Biograph 64 PET-CT scanner; Asahi-Siemens Medical Technologies Ltd., Tokyo, Japan). The duration of the emission scanning using the ECAT HR+ scanner was 10 min. The duration of the transmission scanning using the ECAT HR+ scanner with a $^{68}$Ge/$^{68}$Ga retractable line source was 3 min. This acquisition protocol was the same for both FDG and FMISO. With the Biograph 64 PET-CT scanner, the duration of the emission scanning was also 10 min. The transmission scanning was performed using an X-ray CT, and the attenuation correction used the CT images. The attenuation-corrected radioactivity images from both scanners were reconstructed using a filtered back projection with a 4 mm full width at half maximum Hann filter.

For our second study, to compare the 2-h vs. 4-h images of FMISO PET, we investigated 17 different patients with brain tumors (M/F = 7:10, age $62 \pm 14$ years old, range 33–85 years old). The study populations for first and second studies were

different, and none of the patients included in the first study were included in the second study. The PET images for each patient in the second study were acquired twice, 2 and 4 h following the injection. The injected dosage of FMISO was $399 \pm 25$ MBq. The first scanning took place $115.9 \pm 14.6$ min after the injection and the second $227.4 \pm 15.1$ min after injection. The scanner was a Gemini GXL 16 PET-CT (Philips). The duration of the emission scanning was 20 min. Transmission scanning was performed using the X-ray CT which was used for attenuation correction. Attenuation-corrected radioactivity images were reconstructed using ordered subset expectation maximization.

For the first study, the images were analyzed both qualitatively and quantitatively. An experienced nuclear physician who was blinded from the pathological diagnosis visually evaluated all the images in the qualitative assessment for the first study. In the qualitative assessment of the FMISO PET images, the FMISO uptake was visually categorized into three groups. Where the highest uptake in the tumor was weaker than that in the surrounding brain tissue, the patient was considered as showing *low FMISO uptake*. Where the highest uptake in the tumor was equal to that in the surrounding brain tissue, the patient was considered as showing *intermediate FMISO uptake*. Where the highest uptake in the tumor was stronger than that in the surrounding brain tissue, the patient was considered as showing *high FMISO uptake*. This grouping rule was however not efficient as no patients were assigned to show *low FMISO uptake*. As a result the *low FMISO uptake* and the *intermediate FMISO uptake* patients were combined in one group of *FMISO-negative* patients. The remaining patients, those assigned to the *high FMISO uptake* group, were designated as *FMISO-positive* patients. This binary division was presented in a previous paper [27]. Similarly, in the qualitative assessment of the FDG PET images, we evaluated the FDG accumulation in the tumor using the grouping detailed elsewhere [14]. First, the FDG uptake was visually categorized into three groups: low, intermediate, and high. Where the highest uptake in the tumor was weaker than or equal to that in the contralateral white matter, the patient was considered as showing *low FDG uptake*. Where the highest uptake in the tumor was stronger than that in the contralateral white matter but weaker than that in the contralateral gray matter, the patient was considered as showing *intermediate FDG uptake*. Where the highest uptake in the tumor was equal to or stronger than that in the contralateral gray matter, the patient was considered as showing *high FDG uptake*. Like the FMISO categorization, the *low FDG uptake* and *intermediate FDG uptake* patients were combined and termed *FDG-negative* patients, and those of *high FDG uptake* were termed FDG-positive patients.

For the second study, the grouping of the FMISO uptake in the tumor was performed slightly differently, here it was visually assessed. The degree of uptake was assigned as either high, medium, or low. Low uptake here means the uptake compared to the surrounding brain tissue.

Such qualitative assessments may be subjective and a quantitative assessment was also made. For the first study, the PET images were coregistered with individual MR images (FLAIR) using a mutual information technique implemented in the NEUROSTAT software package [37, 38]. Then, polygonal regions of interest

(ROI) were manually drawn to enclose the entire tumor on every slice that also included peritumoral edematous regions. The single voxel having the highest radioactivity concentration in the tumor was determined in the PET images using in-house software. The highest radioactivity concentration was used to calculate a maximum standardized uptake value ($SUV_{max}$). A $SUV_{peak}$ value has recently come into use to overcome the shortcomings of $SUV_{max}$. However, the concept of $SUV_{peak}$ is not unique as different researchers use different definitions. Here, we use the term $SUV_{10mm}$ to explicitly show the meaning: a 10-mm-diameter circular ROI with the center at the maximum voxel was created. The averaged value for the circular ROI was assigned as $SUV_{10mm}$, and the SUV was calculated as (tissue radioactivity [Bq/ml])*(body weight [g])/(injected radioactivity [Bq]). Next, further ROIs were created on the following reference regions: the cerebellar cortex, the contralateral frontoparietal cortex on the level of the centrum semiovale, and the contralateral frontoparietal white matter on the level of the centrum semiovale. The lesion-to-cerebellum ratio of the FMISO was determined as the ratio of the $SUV_{10mm}$ to the cerebellar averaged SUV. The lesion-to-gray matter and lesion-to-white matter ratios of the FDG were the ratios of $SUV_{10mm}$ to gray matter and white matter SUV, respectively [13]. The ROI placement process was performed by an experienced nuclear physician, and where the tumor occupied bilateral lobes, the hemisphere with the larger part of the tumor was considered as the tumor side. We further measured the hypoxic tissue volume showing significant FMISO uptake in the tumor with the cerebellum used as the reference tissue for this purpose. The voxels having higher SUV than 1.3 times that of the cerebellar SUV were extracted in the tumoral polygonal ROI described above. No threshold for FMISO uptake volumes has been established, and the 1.3 value was empirically adopted from image segmentation in $^{11}$C-methionine brain PET [31, 39, 40]. The FMISO uptake volumes were expressed as a percentage of the extracted voxels in the whole tumoral ROI.

For the second study, the 2-h and 4-h images were coregistered to CT. To obtain reference values from normal tissue, circular 10-mm-diameter ROIs were defined on gray matter, white matter, and the cerebellar cortex. The $SUV_{mean}$, standard deviation (SD), and coefficient of variation (CV) were measured within these ROIs. To express tumor uptake values, the $SUV_{max}$ and lesion-to-cerebellum ratios were calculated in the same way as in the first study.

In the following, all parametric data are expressed as means $\pm$ SD. The patients with grade III or with less malignant gliomas were grouped together as non-glioblastoma patients to simplify the analysis. The relationship between the histopathological diagnosis and the visual assessment results was examined using Fisher's exact test. The differences in age, tumor size, SUVs, lesion-to-normal tissue ratios, and uptake volume for glioblastoma vs. non-glioblastoma patients were examined using the Mann-Whitney *U*-test. The 2-h vs. 4-h values were compared using paired t-tests; *P*-values smaller than 0.05 were considered statistically significant. The statistical analysis and figure drawing used R 2.14.0 and R 3.1.3 for Windows.

## 18.3 Results

In the first study, 14 patients were diagnosed with glioblastomas and categorized as grade IV in the WHO classification. Among the remaining nine patients, one had anaplastic astrocytoma (grade III), one had anaplastic oligodendroglioma (grade III), three had anaplastic oligoastrocytomas (grade III), one had diffuse astrocytoma (grade II), one had oligodendroglioma (grade II), and two had oligoastrocytomas (grade II). Necrosis was identified in all the glioblastoma patients, while none of the non-glioblastoma patients showed necrosis within the tumor. The age of the glioblastoma patients was $65.5 \pm 9.9$ years, and the age of non-glioblastoma patients was $43.7 \pm 12.2$ years; the age difference was statistically significant ($p < 0.01$). The tumor sizes were measured on FLAIR MR images and were not significantly different for glioblastomas vs. non-glioblastomas ($64.4 \pm 17.5$ mm vs. $77.6 \pm 22.5$ mm in diameter) ($p =$ NS). Gadolinium enhancement was observed in 3/9 non-glioblastoma patients and in14/14 glioblastoma patients. By visual assessment, all of the glioblastoma patients (14/14) were classified as FMISO positive and all of the non-glioblastoma patients as FMISO negative. There was a significant association by Fisher's exact test between the histology (glioblastoma or non-glioblastoma) and FMISO uptake (FMISO positive or FMISO negative) ($p < 0.001$). This visual assessment of the FMISO PET images correctly discriminated glioblastoma patients from non-glioblastoma patients with sensitivity, specificity, and accuracy of 100 %, 100 %, and 100 %, respectively. For the FDG PET results, after excluding a diabetic patient with hyperglycemia at the time of the FDG PET, all glioblastoma patients (13/13) were FDG positive and 3/9 non-glioblastoma patients were FDG positive. This relationship reached statistical difference ($p < 0.01$), but the diagnostic performance of the FDG PET was poorer than the FMISO PET, with sensitivity, specificity, and accuracy being 100 %, 66 %, and 86 %, respectively. Figures 18.1, 18.2, 18.3, 18.4, and 18.5 show representative cases.

In the quantitative assessment of the first study, the $SUV_{max}$ of the FMISO was $3.09 \pm 0.62$ (range, 2.22–4.31) in glioblastoma patients, significantly higher than in non-glioblastoma patients ($1.73 \pm 0.36$; range, 1.36–2.39) ($p < 0.001$). As detailed above, we introduced the $SUV_{10mm}$ term to be able to minimize noise effects. The $SUV_{10mm}$ of FMISO was similar to the $SUV_{max}$ of FMISO, with the values being $3.00 \pm 0.61$ (range, 2.15–4.18), significantly higher than in non-glioblastoma patients ($1.64 \pm 0.38$; range, 1.29–2.35) ($p < 0.001$). The lesion-to-cerebellum ratio of the FMISO (the $SUV_{10mm}$/cerebellar SUV) was higher in the glioblastoma patients ($2.74 \pm 0.60$; range, 1.71–3.81) than in the non-glioblastoma patients ($1.22 \pm 0.06$; range, 1.09–1.29) ($p < 0.001$). The quantitative results of the FDG PET were slightly different from those of the FMISO PET. Here the diabetic patient was also excluded from the analyses of SUV and the lesion-to-normal tissue ratio of the FDG PET. The $SUV_{max}$ of the FDG was not significantly different for the glioblastoma and non-glioblastoma patients ($7.55 \pm 3.72$; range, 4.34–16.38, vs. $8.21 \pm 6.04$; range, 4.75–23.49) ($p = 0.95$). Similarly, the $SUV_{10mm}$ of the

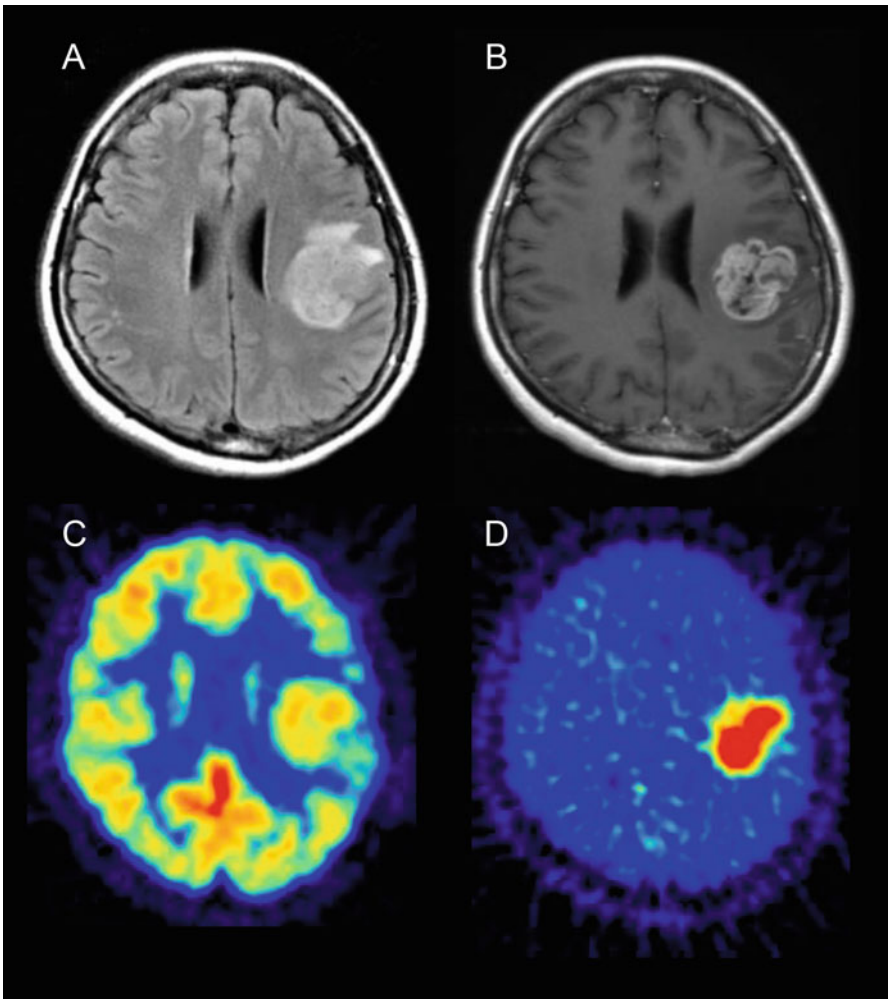


**Fig. 18.1** A glioblastoma case. (**a**) The FLAIR image showed a high-signal tumor in the left hemisphere. (**b**) The tumor was enhanced by gadolinium contrast material. (**c**) The FDG uptake in the tumor was comparable to that of contralateral cerebral cortex. (**d**) The FMISO uptake was higher in the tumor than in the surrounding brain tissue

FDG was not significantly different for the glioblastoma and non-glioblastoma patients ($7.41 \pm 3.63$; range, 4.26–15.90, vs. $8.03 \pm 5.96$; range, 4.64–23.12) ($p = 0.95$). The lesion-to-gray matter ratio of the FDG (the $SUV_{10mm}$/SUV in the contralateral gray matter) was higher in the glioblastoma patients ($1.46 \pm 0.75$; range, 0.91–3.79) than in the non-glioblastoma patients ($1.07 \pm 0.62$; range, 0.66–2.95, $p < 0.05$). The lesion-to-white matter ratio of the FDG (the $SUV_{10mm}$/SUV in the contralateral white matter) was not significantly different for the glioblastoma ($2.81 \pm 1.23$; range, 1.87–6.44) and non-glioblastoma ($2.66 \pm 1.60$;

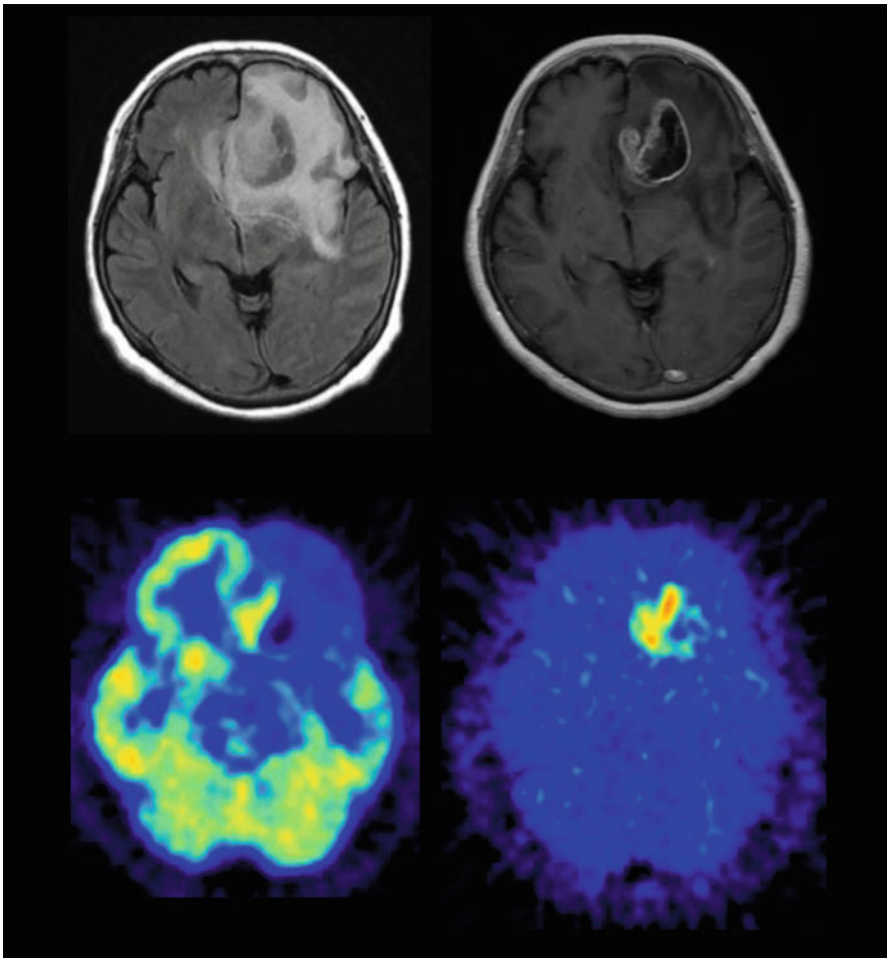

**Fig. 18.2** A glioblastoma case. (**a**) The FLAIR image showed a tumor in the left frontal lobe. (**b**) The tumor showed a ringlike enhancement by gadolinium contrast material. (**c**) The FDG uptake was observed in a part of the gadolinium-enhanced area. The FDG uptake was comparable to the right cerebral cortex. (**d**) The FMISO PET showed a similar distribution of FMISO as FDG but with stronger tumor-to-background contrast than FDG

range, 1.71–6.51) ($p = 0.16$) patients. Finally, the uptake volume of FMISO was larger in the glioblastoma than in non-glioblastoma patients ($27.18 \pm 10.46$ %; range, 14.02–46.67 %, vs. $6.07 \pm 2.50$ %; range, 2.12–9.22 %), ($p < 0.001$).

In the second study, the 2-h images and the 4-h images of FMISO PET were directly compared for the same subjects. Figure 18.6 shows representative images that do not show tumors. Visually, the SUV in the brain was higher at 2 h than at 4 h. More specifically, the gray matter SUV was higher at 2 h than at 4 h, whereas the white matter SUV was comparable in the images at 2 h and 4 h. Profile curves

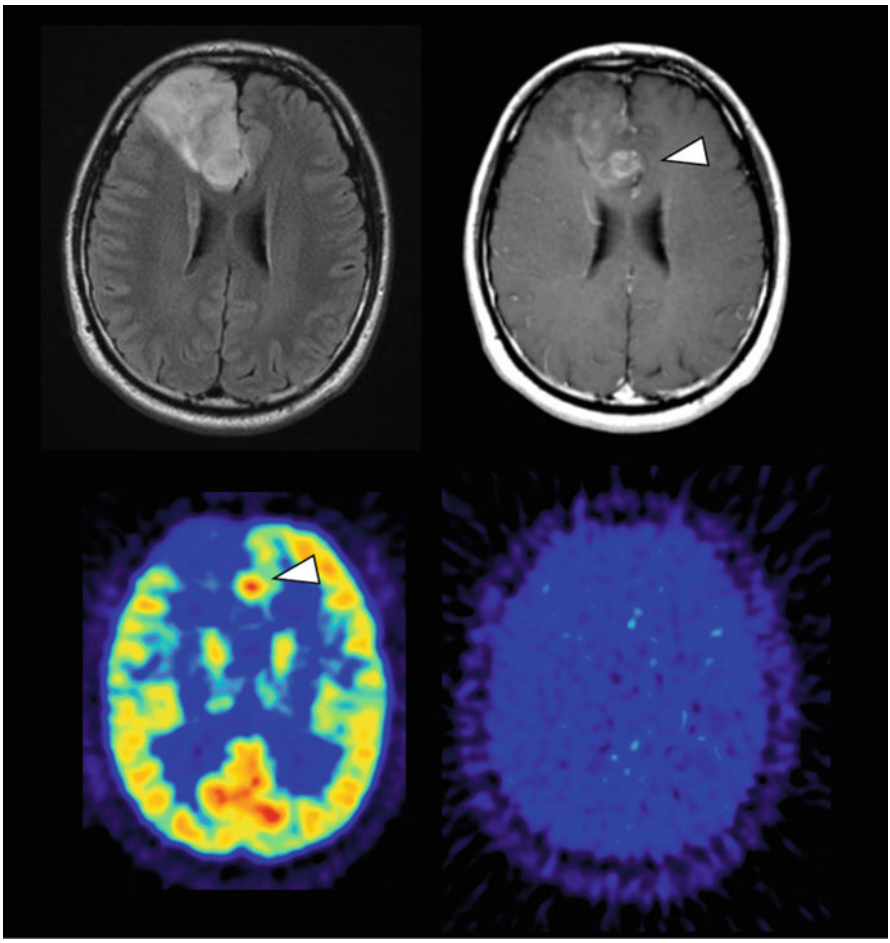

**Fig. 18.3** An anaplastic oligoastrocytoma case (grade III). (**a**) The FLAIR image showed a tumor in the right frontal lobe. (**b**) A small part of the tumor is enhanced after treatment with gadolinium contrast material (arrowhead). (**c**) The FDG uptake was observed in the enhanced part (arrowhead). The FDG uptake was higher than that in the left cerebral cortex. (**d**) No FMISO accumulated in the tumor

demonstrate these differences in Figure 18.6. At 2 h, the gray matter was distinguishable from the white matter, as the gray matter showed higher SUV than the white matter while at 4 h; the curve was almost flat. Figure 18.7 shows scatter plots of gray and white matter SUV at 2 h vs. 4 h. In all cases the gray matter SUV decreased with time and all the points plot under the line of identity. White matter SUV was not significantly different at 2 and 4 h. Figure 18.8 shows the CV of gray and white matter, compared at 2 h and 4 h. The gray matter CV increased slightly from 2 to 4 h ($P = 0.0008$), while the white matter CV was not significantly different at 2 and 4 h.

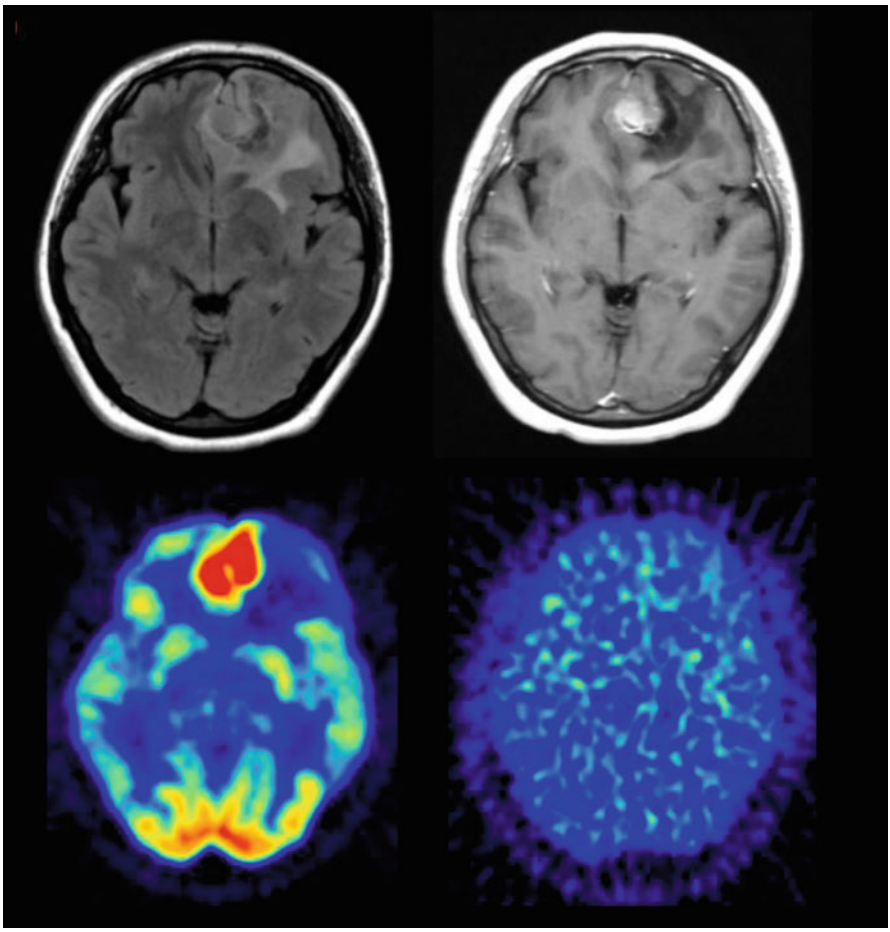

**Fig. 18.4** An anaplastic oligodendroglioma case (grade III). (**a**) The FLAIR image showed a tumor in the left frontal lobe. (**b**) A part of the tumor enhanced by gadolinium contrast material. (**c**) The FDG uptake was observed even outside the enhancing area. The FDG uptake was much higher than that in the right cerebral cortex. (**d**) No FMISO uptake was observed in the tumor

In the visual assessment of the tumors, we first looked into grade IV tumors because based on the first study we believed that the grade IV tumors would have a hypoxic volume and thus should show FMISO uptake. At 2 h, six out of eight grade IV patients showed high FMISO uptakes, and the remaining two patients showed medium uptakes. At 4 h, however, eight out of eight (100 %) patients showed high FMISO uptakes. Then, we looked into grade II and III tumors that we thought would not have developed severe hypoxia and thus would not show FMISO uptake. At 2 h, three out of four patients showed medium uptakes and the fourth patient showed a low uptake. This was changed at 4 h where four out of four (100 %) patients showed low uptakes. The results of the visual assessment can be

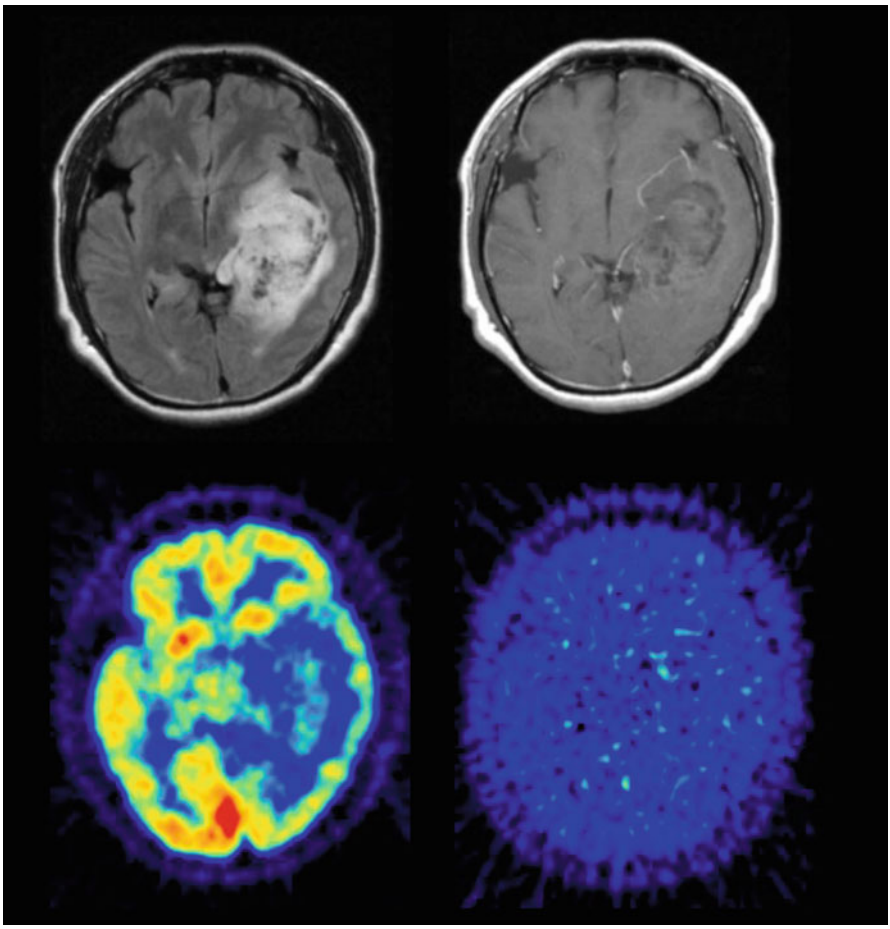

**Fig. 18.5** An oligodendroglioma case (grade II). (**a**) The FLAIR image showed a tumor in the left temporal lobe. (**b**) The tumor slightly enhanced by gadolinium contrast material. (**c**) The FDG uptake was weaker than in the right cerebral cortex. (**d**) No FMISO uptake was observed in the tumor

summarized as those 4-h images provide more definitive information for discriminating grade IV tumors from lower-grade tumors. The quantitative analysis further supported this; in all the cases, the $SUV_{max}$ and tumor-to-normal ratio increased from 2 h to 4 h (Fig. 18.9). Here, lower-grade gliomas (grades II and III) showed decreases in $SUV_{max}$ and in the tumor-to-normal ratio from 2 h to 4 h (Fig. 18.10).

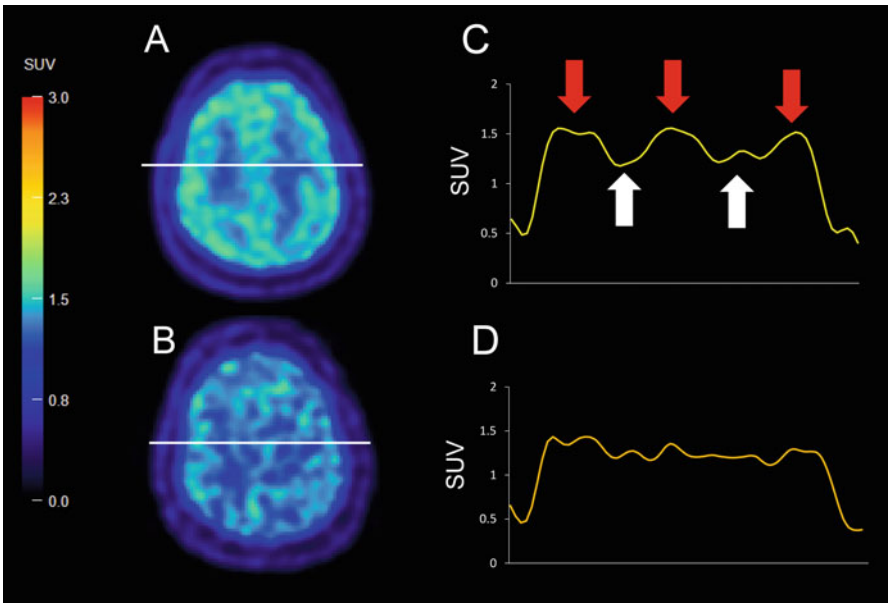


**Fig. 18.6** A brain slice FMISO PET image (**a**) 2 h after administration of FMISO and (**b**) after 4 h. No tumor existed on these slices. (**c**) 2-h SUV profile corresponding to the horizontal line in (**a**). The red arrows indicate gray matter, and the white arrows indicate white matter. (**d**) 4-h profile corresponding to the horizontal line (**b**)

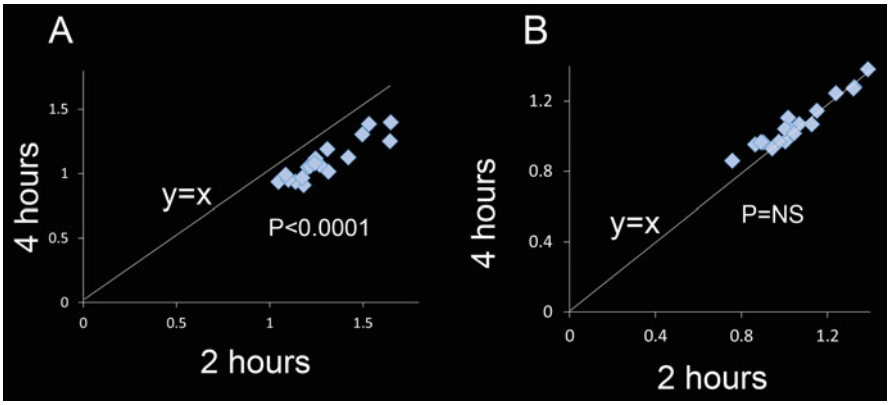


**Fig. 18.7** SUV of (**a**) gray and (**b**) white matter at 2 h vs. 4 h

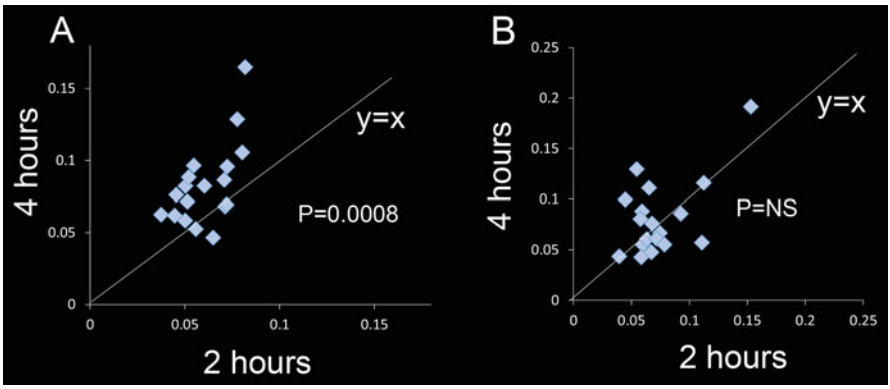


**Fig. 18.8** Plot of variation (CV) of (**a**) gray and (**b**) white matter at 2 h vs. 4 h

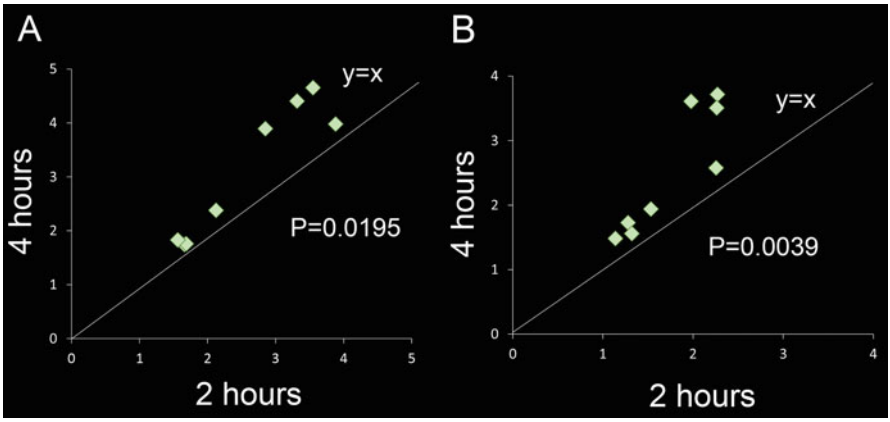


**Fig. 18.9** All glioblastoma cases showed increases in both the (**a**) $SUV_{max}$ and (**b**) tumor-to-normal ratio from 2 h to 4 h

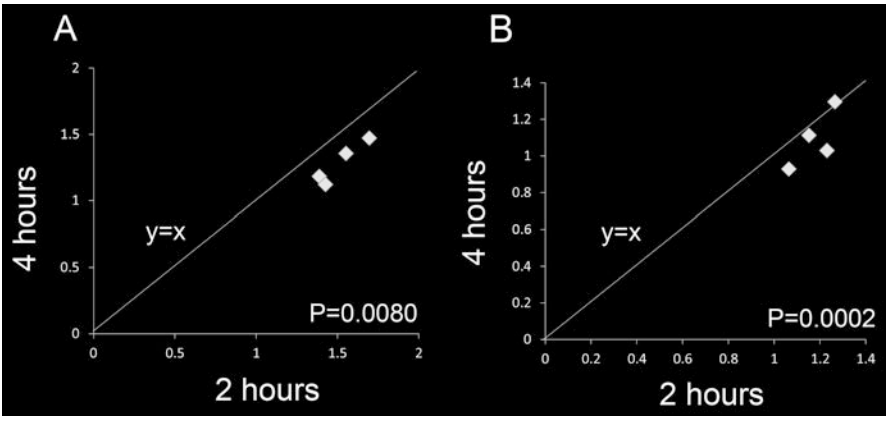


**Fig. 18.10** All grade II to III cases showed decrease in (**a**) $SUV_{max}$, and 3/4 cases showed decrease in (**b**) tumor-to-normal ratio from 2 h to 4 h

## 18.4 Discussion

We have detailed two studies in this article. The results of the first indicated that much FMISO accumulated in all the glioblastomas here but not in the lower-grade gliomas. Different from this, FDG accumulated in both glioblastomas (100 %) and in some lower-grade gliomas (33 %). This suggests that FMISO PET is superior to FDG PET in a differential diagnosis. Visual analysis was confirmed by analyses of the SUV, lesion-to-normal tissue ratio, and FMISO uptake volume. The results of the second study indicated that FMISO PET 4 h after administration is superior to the images after 2 h in differentiating glioblastomas from non-glioblastomas.

In the 2007 WHO definition, grade IV gliomas show microvascular proliferation and necrosis as well as anaplasia and mitotic activity [3]; necrotic tissue is not observed in grade III or lower-grade gliomas. In brain tumor specimens, necrotic change is an important histopathological landmark that distinguishes glioblastomas from lower-grade gliomas. In previous reports, the necrosis in glioblastoma is considered to be associated with tissue hypoxia [16, 17]. The FMISO PET identification of hypoxia proceeds through several steps. Injected FMISO is first transported by the blood flow and taken up by viable cells. Then, FMISO is oxidized by intracellular oxygen if there is a sufficient amount of oxygen available in a cell, and the oxidized FMISO is excreted from the cell. The FMISO is not oxidized when there is insufficient oxygen available (hypoxic conditions) and the FMISO is here retained in the cell [41]. Considering these mechanisms, we may expect that FMISO accumulates in perinecrotic hypoxic tissue but not in the central necrotic region. We observed that only little FMISO accumulates in non-glioblastoma patients. Some studies used needle electrodes to measure oxygen partial pressures in human gliomas [18, 19, 42] and have suggested that both glioblastomas and grade II and III gliomas are present under hypoxic conditions. Lower-grade gliomas do not develop necrosis and may be expected to suffer from only a milder degree of hypoxia than that of glioblastomas [18, 19]. FMISO accumulation requires severe hypoxic conditions ($pO2 < 10$ mmHg) [43, 44], and the results here are consistent with this.

Cher et al. investigated FMISO uptake in various tumors and the correlation with histological findings [27]. They reported that all grade IV tumors showed high FMISO uptakes (they were FMISO positive as we define it here) and that all grade I and II tumors showed FMISO uptakes comparable to the surrounding tissue (they were FMISO negative as we define it). However, there was a slightly elevated FMISO uptake in one of three grade III patients and low uptakes in the remaining two grade III patients [27]. Our results in the first study are consistent with this previous data, except for the grade III patients, as all of our grade III gliomas were FMISO negative. Cher et al. used 2 h as the waiting time before conducting the FMISO PET scanning, while the study here used 4 h. Many FMISO PET protocols have used 2 h as the uptake time [24, 25, 27–32], while Thorwarth et al. questioned the adequacy of 2 h for imaging of FMISO [34]. There, the kinetic analysis of dynamic datasets of FMISO PET suggested that the hot spots at 2 h did not reflect

actual hypoxia but rather showed a high initial influx of the FMISO due to increased blood flow to the tumor. In our first study, no grade III patients showed high FMISO uptakes, and we speculated that this was possibly because the relatively long uptake time allowed the tracer to be excreted from the tissue without severe hypoxia. To further elucidate this, we conducted the second study, to directly compare images at 2 and 4 h after FMISO injection in the same patients. At 4 h, the background gray matter SUV was lower, and the presence of the tumor uptake was fully substantiated: all the glioblastomas were FMISO positive, and all the non-glioblastomas were FMISO negative. These results are consistent with the Thorwarth observations [34].

Recent advances in molecular targeting therapies and image guided therapies are remarkable, and it may be expected that in the near future the therapy of first choice for glioblastomas will be chemo- or radiotherapy rather than surgery. In such cases, new techniques like FMISO PET may help avoid a biopsy followed by a pathological investigation. Aged patients or patients with impaired performance status would particularly benefit from such techniques.

The FDG PET reflects the histological aggressiveness of gliomas, and glioblastomas commonly show the highest FDG uptake among gliomas [12–14]. In the first study here, a high FDG uptake was unexceptionally observed in glioblastoma patients. At the same time, however, three of nine non-glioblastoma patients also showed high FDG uptakes. These findings are consistent with the previous data [13, 14], and the results indicate that FDG PET is useful for histological grading but inconclusive when a differential diagnosis of glioblastomas from lower-grade gliomas is at issue. This leads us to suggest that FMISO PET may play a more important role when a tumor shows a high FDG uptake (equal to or greater than the uptake in the surrounding gray matter). Another important PET tracer for brain tumor imaging is $^{11}$C-methionine (MET). For MET the uptake intensity corresponding to each tumor grade can be summarized as in Fig. 18.11. It is well

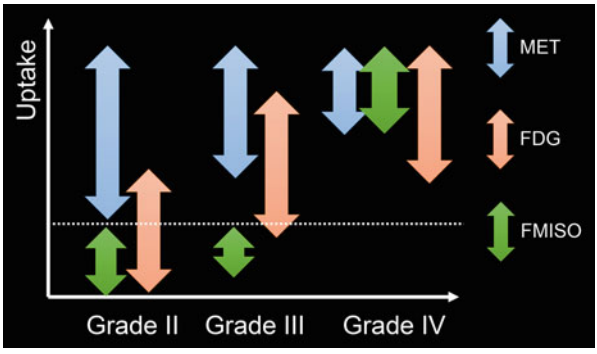


**Fig. 18.11** A scheme of the suggested roles of $^{11}$C-methionine (MET), $^{18}$F-FDG, and $^{18}$F-FMISO PET in differential diagnosis of gliomas

known that even grade II tumors may show high MET uptakes, especially in the case of tumors with oligodendroglial components [45, 46], and that MET is good at showing the tumor boundary. The FDG uptake increases with the tumor grade [47], and the results here suggest that FMISO uptake is absent in grades II and III, but strong in grade IV. Altogether these tracers will provide significant information to assist in distinguishing tumor type and stage.

In the first study, the FMISO PET images were evaluated in different manners by visual assessment, SUV, lesion-to-normal tissue ratio, and uptake volume. The results of these analyses were consistent in showing the relationship between FMISO uptake and glioma grade. In clinical settings the findings suggest that a visual assessment is sufficient for a diagnosis, as the numerical values provide information consistent with the visual assessment. The numerical values may however be useful for purposes like assessing the prognosis and treatment response. Both the $SUV_{max}$ and $SUV_{10mm}$ with FMISO were higher in glioblastoma patients than in non-glioblastoma patients; the range of the values for the groups overlaps, possibly explained by inter-subject variability in the SUV. The lesion-to-cerebellum ratio clearly distinguished glioblastoma patients from non-glioblastoma patients. The usefulness of the lesion-to-cerebellum ratio has also been demonstrated by Bruehlmeier et al. [26], by showing that lesion-to-cerebellum ratios were comparable with the distribution of FMISO volumes. It may be argued that cerebral glioma patients often show asymmetric blood flows in the cerebellum (the so-called crossed cerebellar diaschisis) and that the cerebellar value may not be uniquely useful as a reference. In the study here, FMISO accumulation of the left and right cerebellar cortex did not show significant asymmetry (data not shown); however, this may be assumed not to be a problem in using the lesion-to-cerebellum ratio.

To further confirm the findings, the uptake volume of FMISO in the tumor was measured and compared for glioblastoma and non-glioblastoma patients. This comparison showed that glioblastomas exhibited significantly larger uptake volumes of FMISO than non-glioblastomas. In general, the hypoxic volume is distinguished with tissue-to-blood ratios $\geq 1.2$ in images acquired 2 h after FMISO injection with venous blood samples [28–31]. In brain tumor segmentation for MET PET, a tumor-to-normal ratio $\geq 1.3$ is frequently used [31, 39, 40, 48]. The study here did not collect blood samples at the scanning but showed intratumoral volumes in excess of a 1.3-fold cerebellum mean, which we consider an adequate substitute. The method here did not directly quantify the hypoxic volume, and this is one of the limitations of the study. As another limitation, the number of patients included in this study is small, and further study with more patients is necessary to substantiate the findings. In particular, such studies need to focus on small glioblastoma lesions and aggressive grade III tumors, because these could be a source of false-negative or positive results. Third, we did not investigate specific immunohistochemical features of hypoxia, like the hypoxia-inducible factor-1α (HIF-1α). Investigating HIF-1α further reveals the oxygen condition in the tumor. Finally, in clinical settings, metastatic brain tumors and malignant lymphomas also require a diagnosis that will distinguish them from glioblastomas. Further, additional and different types of brain tumors will need to be investigated.

We also wish to briefly discuss PET tracers other than FMISO [23]. The slow clearance of FMISO from tissue is a shortcoming in clinical settings. If the uptake time could be shortened to maybe 1 h, this would improve the feasibility of hypoxia imaging. Currently, FMISO is the tracer where most evidence has been accumulated, but promising data have been published for other tracers as well. A review article by Kurihara et al. on preclinical and clinical applications of hypoxia PET tracers including FMISO also mentions $^{18}$F-fluoroerythronitroimidazole (FETNIM), $^{18}$F-fluoroazomycin-arabinofuranoside (FAZA), and $^{62}$Cu or $^{64}$Cu-diacetyl-bis($N^4$-methylthiosemicarbazone) (Cu-ATSM) [49]. Among these, FETNIM has not been used with brain tumors, while FAZA is less lipophilic than FMISO, suggesting that background activity in the plasma could be excreted more quickly than FMISO. This point is important for shortening the uptake time. However, in an animal study, Sorger et al. have showed that faster clearance of FAZA resulted in lower FAZA uptake in the tumor than with FMISO [50]. It is not easy to solve this dilemma between uptake time and contrast. Postema et al. conducted a study of FAZA PET in 50 patients with a number of different malignant tumors, including seven glioblastoma patients [51]. Here images were acquired 2–3 h after injection, and the image quality was reported as good, but not superior to FMISO. With Cu-ATSM there is the advantage that the radionuclide $^{62}$Cu can be provided by a $^{62}$Zn/$^{62}$Cu generator, which at present does not require an on-site cyclotron to image hypoxia. O'Donoghue et al. conducted an animal study using a R3327-AT tumor model and found a correlation between the 19-h images of Cu-ATSM and FMISO images at 2–4 h as well as oxygen probe measurements [52]. However, 1-h images of Cu-ATSM did not correlate with the FMISO images. A more recent study by Dence et al. compared Cu-ATSM with FMISO, FDG, and 18 F-fluorothymidine (FLT) using a 9 L gliosarcoma model. Here, autoradiography showed a strong correlation between the Cu-ATSM and FMISO distributions [53]. Tateishi et al. acquired Cu-ATSM PET for glioma patients and demonstrated a correlation between Cu-ATSM uptake and glioma grades [54]. Despite evidence, it is still not substantiated whether Cu-ATSM represents hypoxia. Further, $^{18}$F-EF5, 2-(2-nitro-1[H]-imidazol-1-yl)-N-(2,2,3,3,3-pentafluoropropyl)-acetamide, was first tested in an animal study by Ziemer [55]. Evens et al. found that EF5 uptake correlated with a poor prognosis in glioma patients [18]. They also reported correlations of EF5 uptake with microscopic findings of vasculature [56] and radiation responses [57].

## 18.5 Conclusions

This article summarizes our recent findings in two studies related to FMISO PET for brain tumors. The first study demonstrated that much FMISO accumulated in glioblastomas but not in lower-grade gliomas. The second study demonstrated that FMISO PET images acquired 4 h after administration were better at showing hypoxic tumors than the images acquired 2 h after injection. Combining these

results, the 4-h FMISO PET may be useful in preoperatively discriminating glioblastomas from lower-grade gliomas.



## References

1. Hirata K, Terasaka S, Shiga T, et al. (18)F-Fluoromisonidazole positron emission tomography may differentiate glioblastoma multiforme from less malignant gliomas. Eur J Nucl Med Mol Imaging. 2012;39:760–70.
2. Kobayashi K, Hirata K, Yamaguchi S, et al. FMISO PET at 4 hours showed a better lesion-to-background ratio uptake than 2 hours in brain tumors. J Nucl Med. 2015;56:S373.
3. Louis DN, Ohgaki H, Wiestler OD, et al. The 2007 WHO classification of tumours of the central nervous system. Acta Neuropathol. 2007;114:97–109.
4. Gorlia T, van den Bent MJ, Hegi ME, et al. Nomograms for predicting survival of patients with newly diagnosed glioblastoma: prognostic factor analysis of EORTC and NCIC trial 26981-22981/CE.3. Lancet Oncol. 2008;9:29–38.
5. Cho KH, Kim JY, Lee SH, et al. Simultaneous integrated boost intensity-modulated radiotherapy in patients with high-grade gliomas. Int J Radiat Oncol Biol Phys. 2010;78:390–7.
6. Behin A, Hoang-Xuan K, Carpentier AF, Delattre JY. Primary brain tumours in adults. Lancet. 2003;361:323–31.
7. Spetzler RF, Martin NA. A proposed grading system for arteriovenous malformations. J Neurosurg. 1986;65:476–83.
8. Brasch R, Pham C, Shames D, et al. Assessing tumor angiogenesis using macromolecular MR imaging contrast media. J Magn Reson Imaging. 1997;7:68–74.
9. Law M, Oh S, Babb JS, et al. Low-grade gliomas: dynamic susceptibility-weighted contrast-enhanced perfusion MR imaging--prediction of patient clinical response. Radiology. 2006;238:658–67.
10. Cao Y, Nagesh V, Hamstra D, et al. The extent and severity of vascular leakage as evidence of tumor aggressiveness in high-grade gliomas. Cancer Res. 2006;66:8912–7.
11. Emblem KE, Nedregaard B, Nome T, et al. Glioma grading by using histogram analysis of blood volume heterogeneity from MR-derived cerebral blood volume maps. Radiology. 2008;247:808–17.
12. Di Chiro G, DeLaPaz RL, Brooks RA, et al. Glucose utilization of cerebral gliomas measured by [18F] fluorodeoxyglucose and positron emission tomography. Neurology. 1982;32:1323–9.
13. Kaschten B, Stevenaert A, Sadzot B, et al. Preoperative evaluation of 54 gliomas by PET with fluorine-18-fluorodeoxyglucose and/or carbon-11-methionine. J Nucl Med. 1998;39:778–85.
14. Padma MV, Said S, Jacobs M, et al. Prediction of pathology and survival by FDG PET in gliomas. J Neurooncol. 2003;64:227–37.
15. Borbely K, Nyary I, Toth M, Ericson K, Gulyas B. Optimization of semi-quantification in metabolic PET studies with 18F-fluorodeoxyglucose and 11C-methionine in the determination of malignancy of gliomas. J Neurol Sci. 2006;246:85–94.

16. Oliver L, Olivier C, Marhuenda FB, Campone M, Vallette FM. Hypoxia and the malignant glioma microenvironment: regulation and implications for therapy. Curr Mol Pharmacol. 2009;2:263–84.
17. Flynn JR, Wang L, Gillespie DL, et al. Hypoxia-regulated protein expression, patient characteristics, and preoperative imaging as predictors of survival in adults with glioblastoma multiforme. Cancer. 2008;113:1032–42.
18. Evans SM, Judy KD, Dunphy I, et al. Hypoxia is important in the biology and aggression of human glial brain tumors. Clin Cancer Res. 2004;10:8177–84.
19. Lally BE, Rockwell S, Fischer DB, Collingridge DR, Piepmeier JM, Knisely JP. The interactions of polarographic measurements of oxygen tension and histological grade in human glioma. Cancer J. 2006;12:461–6.
20. Rasey JS, Grunbaum Z, Magee S, et al. Characterization of radiolabeled fluoromisonidazole as a probe for hypoxic cells. Radiat Res. 1987;111:292–304.
21. Martin GV, Caldwell JH, Rasey JS, Grunbaum Z, Cerqueira M, Krohn KA. Enhanced binding of the hypoxic cell marker [3H]fluoromisonidazole in ischemic myocardium. J Nucl Med. 1989;30:194–201.
22. Rasey JS, Koh WJ, Grierson JR, Grunbaum Z, Krohn KA. Radiolabelled fluoromisonidazole as an imaging agent for tumor hypoxia. Int J Radiat Oncol Biol Phys. 1989;17:985–91.
23. Kobayashi H, Hirata K, Yamaguchi S, Terasaka S, Shiga T, Houkin K. Usefulness of FMISO-PET for glioma analysis. Neurol Med Chir (Tokyo). 2013;53:773–8.
24. Valk PE, Mathis CA, Prados MD, Gilbert JC, Budinger TF. Hypoxia in human gliomas: demonstration by PET with fluorine-18-fluoromisonidazole. J Nucl Med. 1992;33:2133–7.
25. Rajendran JG, Mankoff DA, O'Sullivan F, et al. Hypoxia and glucose metabolism in malignant tumors: evaluation by [18F]fluoromisonidazole and [18F]fluorodeoxyglucose positron emission tomography imaging. Clin Cancer Res. 2004;10:2245–52.
26. Bruehlmeier M, Roelcke U, Schubiger PA, Ametamey SM. Assessment of hypoxia and perfusion in human brain tumors using PET with 18F-fluoromisonidazole and 15O-H2O. J Nucl Med. 2004;45:1851–9.
27. Cher LM, Murone C, Lawrentschuk N, et al. Correlation of hypoxic cell fraction and angiogenesis with glucose metabolic rate in gliomas using 18F-fluoromisonidazole, 18F-FDG PET, and immunohistochemical studies. J Nucl Med. 2006;47:410–8.
28. Spence AM, Muzi M, Swanson KR, et al. Regional hypoxia in glioblastoma multiforme quantified with [18F]fluoromisonidazole positron emission tomography before radiotherapy: correlation with time to progression and survival. Clin Cancer Res. 2008;14:2623–30.
29. Swanson KR, Chakraborty G, Wang CH, et al. Complementary but distinct roles for MRI and 18F-fluoromisonidazole PET in the assessment of human glioblastomas. J Nucl Med. 2009;50:36–44.
30. Szeto MD, Chakraborty G, Hadley J, et al. Quantitative metrics of net proliferation and invasion link biological aggressiveness assessed by MRI with hypoxia assessed by FMISO-PET in newly diagnosed glioblastomas. Cancer Res. 2009;69:4502–9.
31. Kawai N, Maeda Y, Kudomi N, et al. Correlation of biological aggressiveness assessed by 11C-methionine PET and hypoxic burden assessed by 18F-fluoromisonidazole PET in newly diagnosed glioblastoma. Eur J Nucl Med Mol Imaging. 2011;38:441–50.
32. Yamamoto Y, Maeda Y, Kawai N, et al. Hypoxia assessed by 18F-fluoromisonidazole positron emission tomography in newly diagnosed gliomas. Nucl Med Commun. 2012;33:621–5.
33. Grunbaum Z, Freauff SJ, Krohn KA, Wilbur DS, Magee S, Rasey JS. Synthesis and characterization of congeners of misonidazole for imaging hypoxia. J Nucl Med. 1987;28:68–75.
34. Thorwarth D, Eschmann SM, Paulsen F, Alber M. A kinetic model for dynamic [18F]-Fmiso PET data to analyse tumour hypoxia. Phys Med Biol. 2005;50:2209–24.
35. Oh SJ, Chi DY, Mosdzianowski C, et al. Fully automated synthesis of [18F]fluoromisonidazole using a conventional [18F]FDG module. Nucl Med Biol. 2005;32:899–905.
36. Tang G, Wang M, Tang X, Gan M, Luo L. Fully automated one-pot synthesis of [18F] fluoromisonidazole. Nucl Med Biol. 2005;32:553–8.

37. Minoshima S, Frey KA, Koeppe RA, Foster NL, Kuhl DE. A diagnostic approach in Alzheimer's disease using three-dimensional stereotactic surface projections of fluorine-18-FDG PET. J Nucl Med. 1995;36:1238–48.
38. Minoshima S, Koeppe RA, Frey KA, Kuhl DE. Anatomic standardization: linear scaling and nonlinear warping of functional brain images. J Nucl Med. 1994;35:1528–37.
39. Kracht LW, Miletic H, Busch S, et al. Delineation of brain tumor extent with [11C]L-methionine positron emission tomography: local comparison with stereotactic histopathology. Clin Cancer Res. 2004;10:7163–70.
40. Galldiks N, Ullrich R, Schroeter M, Fink GR, Jacobs AH, Kracht LW. Volumetry of [(11)C]-methionine PET uptake and MRI contrast enhancement in patients with recurrent glioblastoma multiforme. Eur J Nucl Med Mol Imaging. 2010;37:84–92.
41. Lee ST, Scott AM. Hypoxia positron emission tomography imaging with 18f-fluoromisonidazole. Semin Nucl Med. 2007;37:451–61.
42. Collingridge DR, Piepmeier JM, Rockwell S, Knisely JP. Polarographic measurements of oxygen tension in human glioma and surrounding peritumoural brain tissue. Radiother Oncol. 1999;53:127–31.
43. Koch CJ, Evans SM. Non-invasive PET and SPECT imaging of tissue hypoxia using isotopically labeled 2-nitroimidazoles. Adv Exp Med Biol. 2003;510:285–92.
44. Rasey JS, Nelson NJ, Chin L, Evans ML, Grunbaum Z. Characteristics of the binding of labeled fluoromisonidazole in cells in vitro. Radiat Res. 1990;122:301–8.
45. Kato T, Shinoda J, Oka N, et al. Analysis of 11C-methionine uptake in low-grade gliomas and correlation with proliferative activity. AJNR Am J Neuroradiol. 2008;29:1867–71.
46. Manabe O, Hattori N, Yamaguchi S, et al. Oligodendroglial component complicates the prediction of tumour grading with metabolic imaging. Eur J Nucl Med Mol Imaging. 2015;42:896–904.
47. Yamaguchi S, Terasaka S, Kobayashi H, et al. Combined use of positron emission tomography with (18)F-fluorodeoxyglucose and (11)C-methionine for preoperative evaluation of gliomas. No Shinkei Geka. 2010;38:621–8.
48. Kobayashi K, Hirata K, Yamaguchi S, et al. Prognostic value of volume-based measurements on (11)C-methionine PET in glioma patients. Eur J Nucl Med Mol Imaging. 2015;42:1071–80.
49. Kurihara H, Honda N, Kono Y, Arai Y. Radiolabelled agents for PET imaging of tumor hypoxia. Curr Med Chem. 2012;19:3282–9.
50. Sorger D, Patt M, Kumar P, et al. [18F]Fluoroazomycinarabinofuranoside (18FAZA) and [18F]Fluoromisonidazole (18FMISO): a comparative study of their selective uptake in hypoxic cells and PET imaging in experimental rat tumors. Nucl Med Biol. 2003;30:317–26.
51. Postema EJ, McEwan AJ, Riauka TA, et al. Initial results of hypoxia imaging using 1-alpha-D: −(5-deoxy-5-[18F]-fluoroarabinofuranosyl)-2-nitroimidazole (18F-FAZA). Eur J Nucl Med Mol Imaging. 2009;36:1565–73.
52. O'Donoghue JA, Zanzonico P, Pugachev A, et al. Assessment of regional tumor hypoxia using 18F-fluoromisonidazole and 64Cu(II)-diacetyl-bis(N4-methylthiosemicarbazone) positron emission tomography: Comparative study featuring microPET imaging, Po2 probe measurement, autoradiography, and fluorescent microscopy in the R3327-AT and FaDu rat tumor models. Int J Radiat Oncol Biol Phys. 2005;61:1493–502.
53. Dence CS, Ponde DE, Welch MJ, Lewis JS. Autoradiographic and small-animal PET comparisons between (18)F-FMISO, (18)F-FDG, (18)F-FLT and the hypoxic selective (64)Cu-ATSM in a rodent model of cancer. Nucl Med Biol. 2008;35:713–20.
54. Tateishi K, Tateishi U, Sato M, et al. Application of 62Cu-diacetyl-bis (N4-methylthiosemicarbazone) PET imaging to predict highly malignant tumor grades and hypoxia-inducible factor-1alpha expression in patients with glioma. AJNR Am J Neuroradiol. 2013;34:92–9.
55. Ziemer LS, Evans SM, Kachur AV, et al. Noninvasive imaging of tumor hypoxia in rats using the 2-nitroimidazole 18F-EF5. Eur J Nucl Med Mol Imaging. 2003;30:259–66.
56. Evans SM, Jenkins KW, Jenkins WT, et al. Imaging and analytical methods as applied to the evaluation of vasculature and hypoxia in human brain tumors. Radiat Res. 2008;170:677–90.
57. Koch CJ, Shuman AL, Jenkins WT, et al. The radiation response of cells from 9L gliosarcoma tumours is correlated with [F18]-EF5 uptake. Int J Radiat Biol. 2009;85:1137–47.